Application of the Multiple Scattering Theory to Cloud-Chamber Measurements. I*

STANISLAW OLBERT
Department of Physics and Laboratory for Nuclear Science and Engineering, Massachusetts Institute of Technology, Cambridge, Massachusetts

(Received January 14, 1952)

Some questions concerning the application of the multiple scattering theory to the analysis of cloud-chamber pictures are discussed from the theoretical point of view: (a) The Molière theory of multiple scattering is modified by the consideration of the finite nuclear dimensions. It is assumed that the probability of single scattering goes abruptly to zero for angles greater than $\varphi_0=\varphi_m a/r_n$, where a is the radius of the statistical Thomas-Fermi atom, r_n the radius of the nucleus, and φ_m is the screening angle as derived by Molière. The distribution function for plural and multiple scattering is then derived for finite values of φ_0. It is shown that the cutoff affects especially the tail behavior of the distribution function as it was to be expected. While Molière's function decreases as φ^{-3} for projected angles of scattering large compared to the rms angle, the modified function decreases approximately as $(1/\varphi)$ times a Gaussian function of $(\varphi-\varphi_0)$ for angles large compared to the rms angle and the cut-off angle. (b) The distribution function for the mean value of the square angle of scattering in n plates of a multiple-plate cloud chamber is derived and compared with the normal χ^2-distribution. (c) The effect of observational errors on the distribution function for multiple scattering is estimated quantitatively and discussed in some detail for the case where the mean-square angle of real scattering is large compared to the variance of the noise level scattering.

I. INTRODUCTION

THE observation of Coulomb scattering along the tracks of charged particles in photographic emulsions has played an important role in the identification of cosmic-ray particles and in the determination of their momentum distribution.

Scattering measurements, if properly interpreted, can also be of great value in the analysis of cloud-chamber pictures. Groetzinger, Berger, and Ribe[1] have discussed, from this point of view, the scattering in the gas of a cloud chamber. In the present paper we propose to investigate some theoretical questions concerning the scattering of charged particles in their passage through the metal plates of a multiple-plate cloud chamber. In subsequent papers we shall describe the application of the scattering method to specific problems.

Coulomb scattering of charged particles in finite thicknesses of matter has been the subject of many theoretical studies. Early investigators[2] have treated the problem in the limiting case of multiple scattering, i.e., they have assumed that the particle undergoes a very large number of very small deflections in traversed layer. They have consequently obtained a Gaussian (normal) distribution for the observed angle of scattering. More recently, Snyder and Scott[3] and Molière[4] have treated the problem in a more rigorous and general manner. They have obtained solutions describing the transition from the limiting case of multiple scattering to the limiting case of single scattering through the intermediate case of plural scattering, where the observed deflection results from a small number of individual scattering events. The distribution functions found by Snyder and Scott and by Molière approach the Gaussian function at small angles, but exhibit a much longer "tail" at large angles. In our discussion we shall make use of Molière's results which are analytical in form. However, the theory of Molière (as well as that of Snyder and Scott) neglects the upper limit to the angle of single scattering determined by the finite size of atomic nuclei. Therefore, this theory overestimates the probability of deflection through large angles. In Part II of this paper we shall modify Molière's theory by taking into consideration the finite nuclear size. The other questions discussed in the present paper include, in Part III, the distribution function for the mean square values of the angles of scattering observed in n plates; in Part IV, the effect of the "noise level" scattering on the observed distribution function.

In the analysis of cloud-chamber pictures, the observed quantity is the projected angle of scattering. Therefore, we shall restrict ourselves to the discussion on the distribution of this variable. The theory may be easily modified for the case of spatial angle of scattering.

II. THE EFFECT OF THE FINITE SIZE OF NUCLEI

(a) The Probability of Single Scattering

Molière has derived the following expression for the probability that a particle suffers a deflection through a projected angle between φ' and $\varphi'+d\varphi'$ in consequence of a single collision occurring in a thickness t of the scattering material:

$$f_1(\varphi')d\varphi'=\tfrac{1}{2}Qd\varphi'/(\varphi'^2+\varphi_m^2)^{\frac{3}{2}}. \tag{1}$$

The symbols in Eq. (1) have the following meaning:

$$Q=4\pi\frac{Nt}{A}\left(\frac{Ze^2}{pc\beta}\right)^2, \tag{2}$$

$$\varphi_m=\frac{1.14m_ecZ^{\frac{1}{3}}}{137p}\left[1.13+3.76\left(\frac{Z}{137\beta}\right)^2\right]^{\frac{1}{2}}, \tag{3}$$

* This work was supported in part by the joint program of the ONR and AEC.
[1] Groetzinger, Berger, and Ribe, Phys. Rev. **77**, 584 (1950).
[2] For a review, see B. Rossi and K. Greisen, Revs. Modern Phys. **13**, 240 (1941).
[3] H. S. Snyder and W. T. Scott, Phys. Rev. **76**, 220 (1949).
[4] G. Molière, Z. Naturforsch. **2a**, 133 (1947); **3a**, 78 (1948).

where p = momentum of scattered particle; $c\beta$ = velocity of scattered particle; Ze = nuclear charge of scattering material; A = atomic weight of scattering material; t = thickness of scattering material in g cm^{-2}; N = Avogadro number; m_e = electron mass. The factor Q is the well-known term occurring in the Rutherford formula. The parameter φ_m is the so-called "screening" angle accounting for the shielding effect of atomic electrons. Molière obtained Eq. (3) by assuming the Thomas-Fermi model of the atom with a nucleus of vanishing radius. We shall take into account in an approximate manner the effect of the finite nuclear dimensions by assuming that the scattering probability is given by Eq. (1) for $\varphi' < \varphi_0$ and is identically zero for $\varphi' > \varphi_0$:

$$\bar{f}_1(\varphi';\varphi_0)d\varphi' = \begin{cases} \frac{1}{2}Qd\varphi'/(\varphi'^2+\varphi_m^2)^{\frac{3}{2}}, & |\varphi'| < \varphi_0 \\ 0, & |\varphi'| > \varphi_0. \end{cases} \quad (4)$$

As a definition for the limiting angle φ_0 we shall use the equation

$$\varphi_0/\varphi_m = a/r_n, \quad (5)$$

where $a = 1.67\times10^4 r_e Z^{-\frac{1}{3}}$ represents the radius of the atom computed from the Fermi-Thomas theory, and r_n is of the order of the nuclear radius $R_n = \frac{1}{2}r_e A^{\frac{1}{3}}$ $(r_e = e^2/m_e c^2)$. In the classical limit, $(Z/137\beta)^2 \gg 1$, φ_0, as defined by Eq. (5), tends to the value $2Z(r_e/r_n)$ $(m_e c/p\beta)$, which represents the angle of deflection corresponding to a collision with impact parameter r_n. At the limit for $(Z/137\beta)^2 \ll 1$, φ_0 becomes practically equal to the value $\lambda\!\!\!^{-}/r_n$ in agreement with the results of Born's approximation.

It is convenient to use the Fourier representation for the expression (4):

$$\bar{f}_1(\varphi';\varphi_0) = \frac{1}{2\pi}\int_{-\infty}^{+\infty} d\xi e^{i\xi\varphi'} g(\xi;\varphi_0), \quad (6)$$

with the Fourier transform

$$g(\xi;\varphi_0) = Q\left[\frac{1}{2}\int_{-\infty}^{+\infty}\frac{e^{-i\xi\varphi'}d\varphi'}{(\varphi'^2+\varphi_m^2)^{\frac{3}{2}}} - \int_{\varphi_0}^{+\infty}\frac{\cos(\xi\varphi')d\varphi'}{\varphi'^3}\right], \quad (7)$$

wherein we made use of the fact that $\varphi_0 \gg \varphi_m$.

The evaluation of the first integral in Eq. (7) is discussed in detail by Molière. As one may easily verify, expansion in powers of φ_m yields with sufficient accuracy

$$\frac{1}{2}Q\int_{-\infty}^{+\infty}\frac{e^{-i\xi\varphi'}d\varphi'}{(\varphi'^2+\varphi_m^2)^{\frac{3}{2}}} \approx Q\left[\frac{1}{\varphi_m^2} + \frac{\xi^2}{4}\ln\left(\frac{\gamma^2\varphi_m^2}{4e}\xi^2\right)\right],$$

where $\ln(\gamma^2/e) = 0.154\cdots$ ($ln\gamma$ = Euler's constant).

Hence, the Fourier transform may be written as follows:

$$g(\xi;\varphi_0) = Q\left[\frac{1}{\varphi_m^2} + \frac{\xi^2}{4}\ln\left(\frac{\gamma^2\varphi_m^2}{4e}\xi^2\right) - \int_{\varphi_0}^{+\infty}\frac{\cos(\xi\varphi')d\varphi'}{\varphi'^3}\right]. \quad (8)$$

(b) The Distribution Function for Plural and Multiple Scattering

In order to derive the distribution function we follow a method analogous to that used by Molière.

Let the probability that a particle will suffer a deflection through an angle φ' and $\varphi'+d\varphi'$, as a result of one single scattering, be given by Eq. (6); then the probability that the same particle will be deflected through an angle between $\varphi^{(k)}$ and $\varphi^{(k)}+d\varphi^{(k)}$, as a result of k scattering collisions, is given by

$$\bar{f}_k(\varphi^{(k)};\varphi_0)d\varphi^{(k)} = \frac{d\varphi^{(k)}e^{-g_0}}{2\pi k!}\int_{-\infty}^{+\infty} d\xi \exp(i\xi\varphi^{(k)})[g(\xi;\varphi_0)]^k, \quad (9)$$

where $g_0 \equiv g(0;\varphi_0)$. Therefore, the total probability that the particle will suffer a deflection through an angle between φ and $\varphi+d\varphi$, as a result of the accumulation of 0, 1, 2, $\cdots$, k, scattering collisions is given by the sum of Eq. (9). One thus obtains

$$\bar{f}(\varphi;\varphi_0)d\varphi = \frac{d\varphi e^{-g_0}}{2\pi}\int_{-\infty}^{+\infty} d\xi e^{i\xi\varphi} e^{g(\xi;\varphi_0)}. \quad (10)$$

One may verify that the factor e^{-g_0} normalizes Eq. (10) so that

$$\int_{-\infty}^{+\infty} d\varphi \bar{f}(\varphi;\varphi_0) = 1.$$

Substituting for $g(\xi;\varphi_0)$ the expression (8) and taking into account that $g_0 = Q(1/\varphi_m^2 - 1/2\varphi_0^2)$, one arrives at the following expression for the distribution function:

$$\bar{f}(\varphi;\varphi_0) = \frac{1}{2\pi}\int_{-\infty}^{+\infty} d\xi e^{i\xi\varphi}\exp\left\{Q\left[\frac{\xi^2}{4}\ln\left(\frac{\gamma^2\varphi_m^2}{4e}\xi^2\right) + \frac{1}{2\varphi_0^2} - \int_{\varphi_0}^{\infty}\frac{\cos(\xi\varphi')}{\varphi'^3}d\varphi'\right]\right\}. \quad (11)$$

It now remains to evaluate the integral in Eq. (11). For this purpose it is convenient to introduce with Molière a new dimensionless parameter G, defined by the transcendental equation

$$G = -\tfrac{1}{2}\ln\left(\frac{\gamma^2}{e}\frac{\varphi_m^2}{2GQ}\right). \quad (12)$$

In addition, let us transform simultaneously the variables φ and ξ into the new variables

$$x = \varphi/(2GQ)^{\frac{1}{2}} \quad \text{and} \quad \eta = (2GQ)^{\frac{1}{2}}\xi.$$

Our new scattering variable x represents, therefore, a projected angle measured in units of the characteristic parameter $(2GQ)^{\frac{1}{2}}$. We shall denote this important quantity by $\sqrt{2}\sigma$, referring it thereby to the standard deviation of the normal distribution. The reason for it will become evident later. After a few simple algebraic operations one then finds the following distribution function for the scattering variable x:

$$f(x;x_0)=\frac{1}{2\pi}\int_{-\infty}^{+\infty}d\eta e^{i\eta x}\exp\left[-\frac{\eta^2}{4}+\frac{1}{2G}\left(\frac{\eta^2}{4}\ln\frac{\eta^2}{4}+\frac{1}{2x_0^2}-\int_{x_0}^{\infty}\frac{\cos(\eta x')dx'}{x'^3}\right)\right], \quad (13)$$

where $x_0=\varphi_0/\sqrt{2}\sigma$.

While Eq. (11) is characterized by the three parameters Q, φ_m, and φ_0, note that Eq. (13) is characterized by the three different parameters σ, G, and x_0.

By solving numerically the transcendental Eq. (12), one finds that G may be represented with sufficient accuracy by the explicit expression[5]

$$G\simeq 5.66+1.24\log_{10}\left[\frac{Z^{4/3}A^{-1}t}{1.13\beta^2+3.76(Z/137)^2}\right], \quad (14)$$

for $t>0.1$ g cm^{-2}. Note that G depends not only on the thickness and the atomic number of the scattering material, but also on the velocity of the scattered particle. However, for heavy materials, the dependence on β is slight, e.g., one finds for $\frac{1}{4}$ inch of lead

$$G_0\simeq 6.89 \text{ for } \beta=0, \quad\text{and}\quad G_1\simeq 6.56 \text{ for } \beta=1.$$

Since, in general, G is appreciably larger than unity, we can expand the exponential in Eq. (13) in powers of $(1/2G)$ and neglect terms containing powers higher than the first. After having performed some integrations on the right-hand side of Eq. (13), we find the following approximate expression for $f(x;x_0)$:

$$f(x;x_0)=\exp(-x^2)/\sqrt{\pi}+(1/4G)[f^{(1)}(x;\infty)-\kappa(x;x_0)], \quad (15)$$

where we have used the following abbreviations:

$$f^{(1)}(x;\infty)=\frac{1}{\pi}\int_{-\infty}^{+\infty}d\eta\exp(i\eta x-\eta^2/4)\left(\frac{\eta^2}{4}\ln\frac{\eta^2}{4}\right), \quad (16)$$

$$\kappa(x;x_0)=\frac{2}{\sqrt{\pi}}\exp(-x^2)\left[\int_{x_0}^{\infty}\frac{dx'}{x'^3}\times\exp(-x'^2)\cosh(2xx')-\frac{1}{2x_0^2}\right]. \quad (16')$$

The first term in Eq. (15) is the properly normalized Gaussian. It is predominant for $x<1$, i.e., for angles smaller than $\sqrt{2}\sigma$, since the correction functions $f^{(1)}(x;\infty)$ and $\kappa(x;x_0)$ do not exceed unity, as we shall see later on.

[5] The straight-line relation between G and $\log t$ has been pointed out independently and discussed more exhaustively by W. T. Scott, Phys. Rev. **85**, 245 (1952).

One easily verifies that $f(x;x_0)$ is normalized in such a way that

$$\int_{-\infty}^{+\infty}f(x;x_0)dx=1.$$

The function $f^{(1)}(x;\infty)$, defined by Eq. (16), is the first correction function in Molière's theory. Its properties are discussed by Molière. In particular, it has the following expansions in power series:

For small arguments

$$f^{(1)}(x;\infty)=\frac{2}{\sqrt{\pi}}\exp(-x^2)\sum_{\nu=0}^{\infty}a_\nu x^{2\nu}, \quad (17)$$

where

$$a_0=\tfrac{1}{2}\Psi(\tfrac{1}{2})=0.01825;\quad \Psi(z)=\Gamma'(z+1)/\Gamma(z+1);$$

$$a_1=-1-\Psi(\tfrac{1}{2})=-1.0365;$$

$$a_\nu=\frac{\sqrt{\pi}}{2}\frac{1}{\nu(\nu-1)\Gamma(\nu+\frac{1}{2})},\quad \nu=2,3,4,\cdots. \quad (18)$$

For large arguments

$$f^{(1)}(x;\infty)\approx 1/x^3+3/x^5+45/4x^7+\cdots. \quad (19)$$

The correction function $\kappa(x;x_0)$, defined by Eq. (16′), describes the effect of finite size of the nucleus. Note that, as x_0 approaches infinity, $\kappa(x;x_0)$ vanishes, and Eq. (15) becomes identical with the distribution function given by Molière. However, x_0 is large compared to one only for fairly thin layers of light materials. For, according to Eqs. (5), (3), and (2), x_0 is given by

$$x_0=\frac{\varphi_0}{(2GQ)^{\frac{1}{2}}}\simeq\frac{260}{Z}\left[\frac{A^{\frac{1}{3}}}{Gt}\left(1.13\beta^2+3.76\left(\frac{Z}{137}\right)^2\right)\right]^{\frac{1}{2}}. \quad (20)$$

Equation (20) shows that x_0 is of the order of one for larger values of Z and t, e.g., for $\frac{1}{4}$ inch of lead, one finds that

$$x_0\simeq 1.17(1.19+\beta^2)^{\frac{1}{2}}.$$

In the case of lead, the correction function, $\kappa(x;x_0)$, will modify the Molière distribution appreciably even for angles comparable to σ, as we shall see in the following section.

(c) The Cut-Off Correction Function

We now turn to the calculation of the cut-off correction function, $\kappa(x;x_0)$. By expanding $\cosh(2xx')$ in Eq. (16′) in a power series we obtain the following representation of $\kappa(x;x_0)$:

$$\kappa(x;x_0)=\frac{2}{\sqrt{\pi}}\exp(-x^2)\sum_{\nu=0}^{\infty}b_\nu(x_0)x^{2\nu}, \quad (21)$$

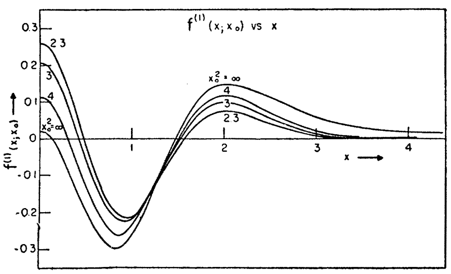

FIG. 1. $f^{(1)}(x;x_0)$ *versus* x for four values of x_0^2: $x_0^2=\infty$; 4; 3; 2.3.

where

$$\begin{aligned} b_0(x_0)&=-\frac{1}{2}\left[\frac{1-\exp(-x_0^2)}{x_0^2}-\mathrm{Ei}(-x_0^2)\right];\\ b_1(x_0)&=-\mathrm{Ei}(-x_0^2);\\ b_\nu(x_0)&=a_\nu[1-I(x_0^2;\nu-2)];\quad \nu=2,3,4,\cdots \end{aligned}\tag{21'}$$

$$-\mathrm{Ei}(-u)=\int_u^\infty e^{-t}t^{-1}dt$$

is the exponential integral; and

$$I(v;p)p!=\int_0^v e^{-t}t^p dt$$

is the incomplete gamma-function.[6]

The similarity between Eqs. (21) and (17) offers the possibility of condensing the functions $f^{(1)}(x;\infty)$ and $\kappa(x;x_0)$ into one expression. By doing so, we obtain a compact form for the distribution function:

$$f(x;x_0)=\exp(-x^2)/\sqrt{\pi}+(1/4G)f^{(1)}(x;x_0),\tag{22}$$

where now

$$f^{(1)}(x;x_0)=\frac{2}{\sqrt{\pi}}\exp(-x^2)\sum_{\nu=0}^{\infty}\alpha_\nu(x_0)x^{2\nu}\tag{23}$$

with the coefficients

$$\begin{aligned} \alpha_0(x_0)&=\frac{1}{2}\left[\Psi(\tfrac{1}{2})+\frac{1-\exp(-x_0^2)}{x_0^2}-\mathrm{Ei}(-x_0^2)\right];\\ \alpha_1(x_0)&=\mathrm{Ei}(-x_0^2)-1-\Psi(\tfrac{1}{2});\\ \alpha_\nu(x_0)&=\frac{\sqrt{\pi}}{2}\frac{I(x_0^2;\nu-2)}{\nu(\nu-1)\Gamma(\nu+\frac{1}{2})},\quad \nu=2,3,4,\cdots. \end{aligned}\tag{23'}$$

The power series in Eq. (23) converges for all values of x. It converges rapidly even for x larger than unity. Equation (23) may, therefore, be used conveniently for mathematical calculations.

Figure 1 shows the behavior of $f^{(1)}(x;x_0)$ for several values of the cut-off parameter x_0. The Molière correction function $f^{(1)}(x;\infty)$ has been drawn for comparison. In all cases, the two correction functions differ markedly from one another for angles appreciably greater than the cut-off angle. Indeed, as we shall prove in the Appendix, for $x\gg x_0$, our correction function becomes

$$f^{(1)}(x;x_0)\approx\frac{1}{2\sqrt{\pi}}\frac{1}{x_0^3x}\exp[-(x-x_0)^2]\times\left[1+\left(x_0+\frac{3}{2x_0}\right)\frac{1}{x}+\cdots\right].\tag{24}$$

It thus drops to zero with increasing x much more rapidly than the Molière correction function which decreases as x^{-3} as x approaches infinity [see Eq. (19)]. Consequently, the "tail" of the distribution function is represented by the equation

$$f(x;x_0)\approx\frac{1}{\sqrt{\pi}}\left\{\exp(-x^2)+\frac{1}{8Gx_0^3x}\exp[-(x-x_0)^2]\times\left[1+\left(x_0+\frac{3}{2x_0}\right)\frac{1}{x}+\cdots\right]\right\}.\tag{25}$$

Among other consequences of the cutoff the following is worth mentioning: The mean-square angle of scattering is no longer infinity as in Molière's theory; for now the expression

$$\langle x^2\rangle_{\mathrm{Av}}\equiv\int_{-\infty}^{+\infty}x^2f(x;x_0)dx\tag{26}$$

converges. Indeed, the substitution of Eqs. (22) and (23) into Eq. (26) and a straightforward integration and summation yield

$$\langle x^2\rangle_{\mathrm{Av}}=\frac{1}{2}\left(\frac{\varphi^2}{\sigma^2}\right)_{\mathrm{Av}}=\frac{1}{2}\left[1+\frac{1}{2G}\{\ln(\gamma x_0^2)-1-\Psi(\tfrac{1}{2})\}\right].\tag{27}$$

Alternately, the mean-square angle can be expressed as

$$\langle\varphi'^2\rangle_{\mathrm{Av}}\equiv\int_{-\varphi_0}^{+\varphi_0}\varphi'^2\bar{f}_1(\varphi';\varphi_0)d\varphi',\tag{28}$$

where $\bar{f}_1(\varphi';\varphi_0)$ is the probability function of single scattering. By virtue of Eq. (4), one finds that

$$\langle\varphi'^2\rangle_{\mathrm{Av}}=Q\left[\frac{1}{2}\ln\frac{\varphi_0+(\varphi_m^2+\varphi_0^2)^{\frac{1}{2}}}{-\varphi_0+(\varphi_m^2+\varphi_0^2)^{\frac{1}{2}}}-\frac{\varphi_0}{(\varphi_m^2+\varphi_0^2)^{\frac{1}{2}}}\right],$$

or, since $\varphi_0\gg\varphi_m$,

$$\langle\varphi'^2\rangle_{\mathrm{Av}}\approx Q[\ln(2\varphi_0/\varphi_m)-1].\tag{29}$$

This is identical with Eq. (27), as one may verify by

[6] See K. Pearson, *Tables of the Incomplete Gamma-Function* (Cambridge University Press, Cambridge, 1946).

remembering that

$$\sigma^2=GQ;\quad x_0^2=\frac{\varphi_0^2}{2\sigma^2};\quad G=-\frac{1}{2}\ln\left(\frac{\gamma^2}{e}\frac{\varphi_m^2}{2\sigma^2}\right);$$

$$\Psi(\tfrac{1}{2})=2-\ln 4\gamma.$$

III. DISTRIBUTION OF MEAN-SQUARE ANGLE

The distribution function derived in Part II can be applied directly to the interpretation of experimental data only when the number of measured angles of scattering is very large and when all measurements refer to particles of the same kind and the same momentum. In this case a fitting of the experimental data to the theoretical distribution curve yields the value of the parameter σ and, therefore, affords a determination of the momentum of the particle. More simply, if $\varphi_1, \varphi_2, \cdots, \varphi_n$ represent the measured angles, the quantity

$$(\varphi^2)_{\mathrm{Av}}\equiv\frac{1}{n}\sum_{i=1}^{n}\varphi_i^2 \tag{30}$$

may be regarded as equal to the mean-square angle, $\langle\varphi^2\rangle_{\mathrm{Av}}$, which is related to σ by Eq. (27).

In the evaluation of cloud-chamber results, however, we are often faced with a different problem. The observed particles have, in general, different momenta and different masses, and each particle goes through a small number of plates. For each particle we may compute the value of $(\varphi^2)_{\mathrm{Av}}$ by means of Eq. (30), but, because of the small value of n, there is no longer a definite relation between the value of $(\varphi^2)_{\mathrm{Av}}$ and the value of σ^2 for the particle in question. From the distribution in the experimental values of $(\varphi^2)_{\mathrm{Av}}$, we wish to derive the maximum amount of information concerning the scattering parameter σ. Clearly, for the solution of this problem, it is necessary to compute the distribution function for the quantity $(\varphi^2)_{\mathrm{Av}}$ in the case of a homogeneous group of particles.

For simplicity, we neglect the momentum loss of the particles in the traversal of the plates and we introduce, instead of $(\varphi^2)_{\mathrm{Av}}$, the quantity

$$\chi^2=\frac{n(\varphi^2)_{\mathrm{Av}}}{2\sigma^2}=\sum_{i=1}^{n}x_i^2. \tag{31}$$

Let $F_n(\chi; x_0)d\chi$ represent the probability that χ lies between χ and $\chi+d\chi$. One may derive the mathematical expression of $F_n(\chi; x_0)$ with the following argument.

The distribution function for each of the n scattering variables x_i is known and is given by Eq. (22). Since we may consider the variables x_i as statistically independent, the probability that x_1 will lie in the interval between x_1 and x_1+dx_1, x_2 in the interval between x_2 and x_2+dx_2, etc., is given by the product of n expressions of the type of Eq. (22), *viz.*,

$$f_n(x_1, \cdots, x_n; x_0)d^nx = f(x_1; x_0)f(x_2; x_0)\cdots f(x_n; x_0)d^nx, \tag{32}$$

where d^nx stands for $dx_1dx_2\cdots dx_n$.

If one interprets the variables x_i as Cartesian coordinates in an n-dimensional space, one immediately sees from Eq. (31) that χ has a constant value over the surface of a hyper-sphere, since χ has the meaning of the radius of this hyper-sphere. Therefore, the probability $F_n(\chi; x_0)d\chi$ is given by the equation

$$F_n(\chi; x_0)d\chi=\int f(x_1; x_0)\cdots f(x_n; x_0)d^nx, \tag{33}$$

where the integration extends over the volume included between the hyper-spheres of radii χ and $\chi+d\chi$. One can easily prove that the following transformation satisfies Eq. (31):

$$\begin{aligned}
x_1&=\chi\cos\beta_1\cos\beta_2\cdots\cos\beta_{n-1},\\
x_2&=\chi\sin\beta_1\cos\beta_2\cdots\cos\beta_{n-1},\\
&\cdots\cdots\cdots\\
x_i&=\chi\sin\beta_{i-1}\cos\beta_i\cdots\cos\beta_{n-1},\\
&\cdots\cdots\cdots\\
x_n&=\chi\sin\beta_{n-1}.
\end{aligned}$$

The β_i, $(i=1, \cdots, n-1)$, are now independent variables with respect to the limits of the integral in Eq. (33). We write for the volume element

$$d^nx=dA\,d\chi,$$

where dA is the surface element on the n-dimensional hyper-sphere, and has the expression

$$dA=\begin{vmatrix}\partial x_1/\partial\chi & \cdots & \partial x_n/\partial\chi\\ \partial x_1/\partial\beta_1 & \cdots & \partial x_n/\partial\beta_1\\ \cdots & \cdots & \cdots\\ \partial x_1/\partial\beta_{n-1} & \cdots & \partial x_n/\partial\beta_{n-1}\end{vmatrix} d\beta_1d\beta_2\cdots d\beta_{n-1}$$
$$=\chi^{n-1}\cos\beta_2\cos^2\beta_3\cdots\cos^{n-2}\beta_{n-1}d\beta_1\cdots d\beta_{n-1}. \tag{34}$$

We can rewrite Eq. (33) as

$$F_n(\chi; x_0)d\chi = d\chi 2^n\int_0^{\pi/2}\cdots\int_0^{\pi/2} f(x_1; x_0)\cdots f(x_n; x_0)dA, \tag{35}$$

where dA is given by Eq. (34). The factor 2^n in Eq. (35) arises from the fact that the integral in Eq. (35) is extended only over the positive part (positive 2^n-ant) of our hyper-sphere. By substituting Eq. (22) for $f(x_i; x_0)$ and neglecting terms proportional to powers of $(1/2G)$ greater than the first, one obtains

$$F_n(\chi; x_0)=\left(\frac{2}{\sqrt{\pi}}\right)^n\exp(-\chi^2)\times\int_0^{\pi/2}\cdots\int_0^{\pi/2}\left(1+\frac{1}{2G}\sum_{i=1}^{n}\sum_{\nu=0}^{\infty}\alpha_\nu(x_0)x_i^{2\nu}\right)dA. \tag{36}$$

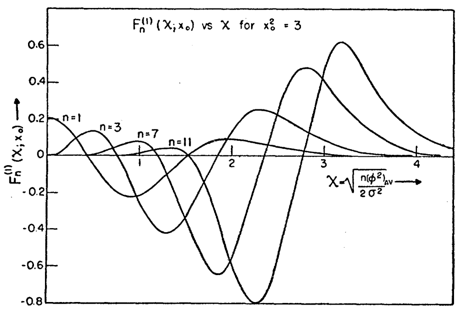

FIG. 2. $F_n^{(1)}(\chi; x_0)$ *versus* χ for $x_0^2=3$, and for four values of n: $n=1, 3, 7, 11$.

The integrals in Eq. (36) are all of the form

$$\int_A x_i^{2\mu}dA=\chi^{2\mu+n-1}\int_0^{\pi/2}\cdots\int_0^{\pi/2}\sin^{2\mu}\beta_{i-1}\cos\beta_i^{2\mu}\cdots \times\cos^{2\mu}\beta_{n-1}\cos\beta_2\cos^2\beta_3\cdots\cos^{n-2}\beta_{n-1}d^{n-1}\beta.$$

This integral has the value

$$\int_A x_i^{2\mu}dA=\chi^{2\mu+n-1}\left(\frac{\sqrt{\pi}}{2}\right)^{n-1}\frac{\Gamma(\mu+\frac{1}{2})}{\Gamma(\mu+\frac{1}{2}n)}. \qquad (37)$$

Note that the right-hand side of Eq. (37) is independent of the index i, so we can replace the sum over i in Eq. (36) by the factor n. By combining Eqs. (37) and (36) one thus obtains

$$F_n(\chi; x_0)=\frac{2}{\Gamma(\frac{1}{2}n)}\chi^{n-1}\exp(-\chi^2) \times\left(1+\frac{1}{2G}\sum_{\nu=0}^{\infty}\alpha_\nu^{(n)}(x_0)\chi^{2\nu}\right), \qquad (38)$$

where

$$\alpha_\nu^{(n)}(x_0)=\frac{2}{\sqrt{\pi}}\frac{\Gamma(1+\frac{1}{2}n)\Gamma(\nu+\frac{1}{2})}{\Gamma(\nu+\frac{1}{2}n)}\alpha_\nu(x_0).$$

The coefficients α_ν are defined by Eqs. (23′). The series in Eq. (38) converges for all χ. Also, it can be shown that F_n is properly normalized, i.e.,

$$\int_0^\infty F_n(\chi; x_0)d\chi=1.$$

The first term in Eq. (38) corresponds to the Gaussian approximation. It is identical with the expression known in the literature as "χ^2-distribution for n degrees of freedom." The second term represents the corrections to this normal distribution. Figure 2 shows the behavior of the correction function

$$F_n^{(1)}(\chi; x_0)=\frac{2}{\Gamma(\frac{1}{2}n)}\chi^{n-1}\exp(-\chi^2)\sum_{\nu=0}^{\infty}\alpha_\nu^{(n)}(x_0)\chi^{2\nu} \qquad (39)$$

for $n=3$, 7, and 11. For the cut-off variable, x_0, we have taken $x_0^2=3$, which is a good approximate value for the $\frac{1}{4}$ inch lead plates. (A very accurate value of x_0 is not necessary since the correction functions $F_n^{(1)}$ are fairly insensitive to x_0.)

Figure 3 shows the deviation of F_n from the normal χ^2-distribution. The ordinate R_n represents the ratio

$$R_n(\chi; x_0)=\frac{[2/\Gamma(\frac{1}{2}n)]\chi^{n-1}\exp(-\chi^2)}{F_n(\chi; x_0)} =\frac{1}{1+(1/2G)\sum\alpha_\nu^{(n)}(x_0)\chi^{2\nu}} \qquad (40)$$

for $2G=13.4$, $x_0^2=3$, and $n=1$, 3, 7, 11. In particular, R_1 represents the ratio of the Gaussian $\exp(-x^2)/\sqrt{\pi}$ to the distribution function $f(x; x_0)$, derived in Part II; ($F_1=2f(x; x_0)$). One sees that in all cases the deviations become significant for $(\varphi^2)_{\text{Av}}>\sigma^2$.

To conclude the discussion on the distribution function F_n, we calculate the position of the maximum of $F_n(\chi; x_0)$. For this purpose we have to solve the equation

$$[\chi^2_{\text{most prob.}}-\tfrac{1}{2}(n-1)]\left(1+\frac{1}{2G}\sum_{\nu=0}^{\infty}\alpha_\nu^{(n)}\chi^{2\nu}_{\text{most prob.}}\right) -\frac{1}{2G}\sum_{\nu=1}^{\infty}\nu\alpha_\nu^{(n)}\chi^{2\nu}_{\text{most prob.}}=0,$$

which follows from the differentiation of Eq. (38). By setting

$$\chi^2_{\text{most prob.}}=\tfrac{1}{2}(n-1)+\omega_n(x_0)/2G \qquad (41)$$

and neglecting terms proportional to $(1/2G)^2$, we find that

$$\omega_n(x_0)=\sum_{\nu=1}^{\infty}\nu\alpha_\nu^{(n)}(x_0)\left(\frac{n-1}{2}\right)^\nu. \qquad (42)$$

Table I gives the numerical values of ω_n for some values of x_0 and n. Combining Eqs. (31), (41), and (42) one thus has the following expression for the most probable value of the rms angle $\sqrt{(\varphi^2)_{\text{Av}}}$:

$$[(\varphi^2)_{\text{Av}}^{\frac{1}{2}}]_{\text{most prob.}}=\left(\frac{n-1}{n}\right)^{\frac{1}{2}}\sigma\left[1+\frac{1}{2G}\frac{\omega_n(x_0)}{n-1}\right]. \qquad (41')$$

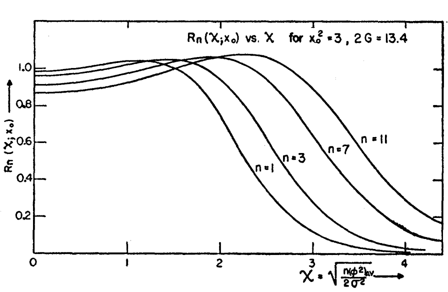

FIG. 3. $R_n(\chi; x_0)$ *versus* χ for $x_0^2=3$, $2G=13.4$, and for four values of n: $n=1, 3, 7, 11$.

IV. "NOISE LEVEL" SCATTERING[7]

We now turn our attention to a different problem that occurs in the theory of multiple scattering. Up to now, we have assumed that the projected angles of deflection corresponding to the scattering in the plates of a cloud chamber can be measured with absolute accuracy. In practice, of course, this is not the case. A cloud-chamber track consists of a discrete array of droplets whose centers do not lie exactly along the trajectory of the ionizing particle. This fact, together with the imperfection of the measuring instruments, introduce errors in the determination of the direction of the track between consecutive plates. These errors result in an apparent scattering that we may term "noise level" scattering.

Let us introduce an arbitrary line of reference, and let γ be the measured value of the angle between this line and the central line of the track. Let $\bar{\gamma}$ be the true value of this angle. The distribution of γ around $\bar{\gamma}$ may be assumed to be normal:

$$N_1(\gamma)=\frac{1}{\sigma_1(2\pi)^{\frac{1}{2}}}\exp\left[-\frac{1}{2\sigma_1^2}(\gamma-\bar{\gamma})^2\right],$$

where σ_1 is the standard deviation corresponding to the noise level scattering.

If we assume that there is no real scattering in any of n plates, the measured $(n+1)$ angles, $\gamma_0, \gamma_1, \cdots, \gamma_n$, between the line of reference and the ith section of the track will obey the $(n+1)$-dimensional normal distribution

$$N_{n+1}(\gamma_0, \cdots, \gamma_n)=\left[\frac{1}{\sigma_1(2\pi)^{\frac{1}{2}}}\right]^{n+1}\exp\left[-\frac{1}{2\sigma_1^2}\sum_{i=0}^{n}(\gamma_i-\bar{\gamma})^2\right]. \quad (43)$$

However, we are not interested in the distribution of the angles γ_i, but rather in the distribution of their consecutive differences, i.e.,

$$\Delta_i=\gamma_i-\gamma_{i-1}.$$

One may derive the n-dimensional distribution function of Δ_i from Eq. (43) by expressing the γ_i in terms of Δ_i. One finds

$$h_n(\Delta_1, \cdots, \Delta_n)=\left(\frac{1}{\sigma_1(2\pi)^{\frac{1}{2}}}\right)^n D_n^{-\frac{1}{2}} \times\exp\left[-\frac{1}{2\sigma_1^2}\sum_{i,k}^{n}a_{ik}^{-1}\Delta_i\Delta_k\right], \quad (44)$$

where a_{ik}^{-1} are the elements of the matrix reciprocal to the following matrix:

$$(a_{ik})=\begin{pmatrix} 2 & -1 & 0 & \cdot & \cdot & 0 \\ -1 & 2 & -1 & 0 & \cdot & 0 \\ 0 & -1 & 2 & -1 & \cdot & 0 \\ \cdot & \cdot & \cdot & \cdot & \cdot & \cdot \\ \cdot & \cdot & \cdot & \cdot & \cdot & \cdot \\ 0 & \cdot & \cdot & \cdot & -1 & 2 \end{pmatrix}$$

and D_n is the determinant of matrix (a_{ik}).

On the other hand, if we disregard the noise level scattering, and consider only the real scattering in n plates, the n-dimensional distribution for the differences φ_i between the angular positions of consecutive segments of the track is described by Eq. (32):

$$\bar{f}_n(\varphi_1, \cdots, \varphi_n; x_0)=\prod_{i=1}^{n}\bar{f}(\varphi_i; x_0), \quad (45)$$

where

$$\bar{f}(\varphi_i; x_0)=\frac{1}{\sigma(2\pi)^{\frac{1}{2}}} \times\exp(-\varphi_i^2/2\sigma^2)\left[1+\frac{1}{4G}\sum_{\nu=0}^{\infty}\alpha_\nu(x_0)\left(\frac{\varphi_i^2}{2\sigma^2}\right)^\nu\right]. \quad (45')$$

We are now in the position to write the complete distribution function for the actually observed angles:

$$\theta_i=\varphi_i+\Delta_i,$$

which include both real scattering and noise level scattering. This distribution function is given by

$$H_n(\theta_1, \cdots, \theta_n)=\int_{-\infty}^{+\infty}\cdots\int_{-\infty}^{+\infty}d^n\Delta \times\bar{f}_n(\theta_1-\Delta_1, \cdots, \theta_n-\Delta_n)h_n(\Delta_1, \cdots, \Delta_n), \quad (46)$$

where $\bar{f}_n$ is defined by Eq. (45), h_n is defined by Eq. (44) and $d^n\Delta$ stands for $d\Delta_1 d\Delta_2\cdots d\Delta_n$. One can integrate Eq. (46) without difficulty in the case where the functions $\bar{f}(\varphi_i, x_0)$ obey the normal distribution, i.e., if one neglects terms involving $(1/2G)$ in Eq. (45′). The result may be written as

$$H_n(\theta_1, \cdots, \theta_n)=\left(\frac{1}{\sigma'(2\pi)^{\frac{1}{2}}}\right)^n D_n'^{-\frac{1}{2}} \times\exp\left[-(1/2\sigma'^2)\sum_{i,k}^{n}A_{ik}^{-1}\theta_i\theta_k\right], \quad (47)$$

TABLE I. Numerical values of $\omega_n(x_0)\equiv 2G[\chi^2{}_{\text{most prob.}}-\frac{1}{2}(n-1)]$.

	$n=3$	$n=7$	$n=11$
$x_0^2=2.3$	-0.667	-0.964	-0.775
$x_0^2=3$	-0.628	-0.694	-0.190

[7] This discussion is based in outline on the theory of noise level scattering in photographic plates developed by G. Molière [*Theorie der Streuung schneller geladener Teilchen, III*, to be published]. It is an adaptation of Molière's theory for the analysis of multiple-plate cloud-chamber pictures.

where now

$$\sigma'^2=(1+2\mu)\sigma^2;\quad \mu=\sigma_1^2/\sigma^2,$$

$$A_{ik}=(\delta_{ik}+\mu a_{ik})/(1+2\mu),\quad \delta_{ik}=\begin{cases}1 & i=k\\ 0 & i\neq k\end{cases};$$

$$D_n'=\det(A_{ik}).$$

Explicitly, one has for A_{ik}

$$(A_{ik})=\begin{bmatrix}1 & -\epsilon & 0 & 0 & \cdot & 0\\ -\epsilon & 1 & -\epsilon & 0 & \cdot & 0\\ 0 & -\epsilon & 1 & -\epsilon & \cdot & 0\\ \cdot & \cdot & \cdot & \cdot & \cdot & \cdot\\ \cdot & \cdot & \cdot & \cdot & \cdot & \cdot\\ 0 & \cdot & \cdot & \cdot & -\epsilon & 1\end{bmatrix}, \tag{48}$$

with $\epsilon=\mu/(1+2\mu)$. Furthermore, note that all parameters in Eq. (47), i.e., σ', D_n', A_{ik}, are expressed in terms of one quantity μ. If μ approaches zero, H_n approaches the distribution function $\bar{f}_n$ computed under the Gaussian approximation, i.e., the function

$$\bar{f}_n(\varphi_1,\cdots,\varphi_n)=\left(\frac{1}{\sigma(2\pi)^{\frac{1}{2}}}\right)^n\exp\left[-\frac{1}{2\sigma^2}\sum_{i=1}^n\varphi_i^2\right].$$

Explicit formulas for D_n' and the reciprocal matrix elements A_{ik}^{-1} may be calculated from the matrix (48). Because of its complicated character we shall omit this computation and limit ourselves to one special case

$$\mu\ll 1,$$

i.e., we assume that the noise level scattering is much smaller than the real scattering. In this case

$$\epsilon\approx\mu;\quad (A_{ik}^{-1})\approx\begin{bmatrix}1 & \mu & 0 & 0 & \cdot & 0\\ \mu & 1 & \mu & 0 & \cdot & 0\\ 0 & \mu & 1 & \mu & \cdot & 0\\ \cdot & \cdot & \cdot & \cdot & \cdot & \cdot\\ \cdot & \cdot & \cdot & \cdot & \cdot & \cdot\\ 0 & \cdot & \cdot & \cdot & \mu & 1\end{bmatrix},$$

and $D_n'\approx 1$, so that the expression in the exponent of Eq. (47) becomes simply

$$\sum_{i,k}^n A_{ik}^{-1}\theta_i\theta_k\approx\theta_1^2+\theta_2^2+\cdots+\theta_n^2 +2\mu(\theta_1\theta_2+\theta_2\theta_3+\cdots+\theta_{n-1}\theta_n).$$

Hence we may write for Eq. (47)

$$H_n(\theta_1,\cdots,\theta_n)\approx\left(\frac{1}{\sigma'(2\pi)^{\frac{1}{2}}}\right)^n\exp\left[-\frac{1}{2\sigma'^2}\sum_{i=1}^n\theta_i^2\right] \times\left[1-\frac{\mu}{\sigma'^2}(\theta_1\theta_2+\cdots+\theta_{n-1}\theta_n)\right]. \tag{49}$$

From Eq. (49) one can see that the noise level scattering has two effects. First, it increases the standard deviation from the value σ to the value

$$\sigma'\approx(1+\mu)\sigma.$$

Secondly, it introduces a statistical correlation between the consecutive angles θ_i and θ_{i+1}. The n-dimensional distribution function can no longer be expressed as a product of Gaussians, i.e., the scattering angles are no longer statistically independent. However, one may verify that the distribution function for the root-mean-square angle $(\theta^2)_{\text{Av}}^{\frac{1}{2}}$ is not affected by the correlation mentioned above. An integration of H_n, similar to that discussed in Part III, yields the following distribution for $\chi'=[n(\theta^2)_{\text{Av}}/2\sigma'^2]^{\frac{1}{2}}$:

$$F_n'(\chi';x_0)d\chi'\approx\frac{2}{\Gamma(\frac{1}{2}n)}\chi'^{n-1}\exp(-\chi'^2) \times\left[1+\frac{1}{2G}\sum\alpha_\nu^{(n)}(x_0)\chi'^{2\nu}+\cdots\right],$$

i.e., $(\theta^2)_{\text{Av}}$ is distributed in the same manner as $(\varphi^2)_{\text{Av}}$ but has a different standard deviation. The latter fact affects the position of the maximum of the distribution in rms angle. We now have for small μ

$$[(\theta^2)_{\text{Av}}^{\frac{1}{2}}]_{\text{most prob.}}=(1+\mu)[(\varphi^2)_{\text{Av}}^{\frac{1}{2}}]_{\text{most prob.}},$$

where $[(\varphi^2)_{\text{Av}}^{\frac{1}{2}}]_{\text{most prob.}}$ is given by Eq. (41').

The noise level scattering also modifies the expression (29), *viz.*,

$$\langle\theta^2\rangle_{\text{Av}}=(1+2\mu)Q[\ln(2\varphi_0/\varphi_m)-1].$$

The author wishes to express his gratitude to Professor B. Rossi for his great interest and active help in the preparation of this paper, and to Dr. W. T. Scott for his review and criticism of the manuscript.

APPENDIX

The representation of the correction function $f^{(1)}(x;x_0)$ in power series of x, as given by Eq. (23), is inconvenient for the study of the behavior of this function for large arguments. In order to find the asymptotic expansion of $f^{(1)}(x;x_0)$ for $x\gg 1$ we rewrite the correction function as follows:

$$f^{(1)}(x;x_0)=\frac{2}{\sqrt{\pi}}\exp(-x^2)\left[\alpha_0+\alpha_1x^2 +\sum_{k=0}^\infty(-1)^k\frac{x_0^{2k-2}}{k!}w_k(z),\right. \tag{A1}$$

where $z=2xx_0$ and

$$w_k(z)=\frac{1}{2}\sum_{\nu=2}^\infty\frac{z^{2\nu}}{(2\nu)!(\nu-1+k)}. \tag{A2}$$

One may verify the correctness of the above expressions by making use of the following formula:

$$I(x_0^2;\,\nu-2)=\frac{1}{(\nu-2)!}\sum_{k=0}^{\infty}(-1)^k\frac{x_0^{2k+2\nu-2}}{k!(\nu-1+k)}. \quad \text{(A3)}$$

By virtue of the known theorem

$$\frac{1}{(2\nu)!}=\frac{1}{2\pi i}\int_\gamma e^t t^{-2\nu-1}dt$$

(where γ represents any integration path encircling the origin once in a counter clockwise direction), we may express Eq. (A2) as follows:

$$w_k(z)=\frac{1}{2z}\frac{1}{2\pi i}\int_\gamma dt e^t \sum_{\nu=2}^{\infty}\left(\frac{z}{t}\right)^{2\nu+1}\frac{1}{k+\nu-1}. \quad \text{(A4)}$$

If we choose the integration path so that $|z/t|<1$, we may sum up the series in Eq. (A4) as

$$\sum_{\nu=2}^{\infty}\left(\frac{z}{t}\right)^{2\nu+1}\frac{1}{\nu+k-1}=-\left(\frac{z}{t}\right)^{3-2k}\left[\ln\left(1-\frac{z^2}{t^2}\right)+p_k\left(\frac{z}{t}\right)\right],$$

where

$$p_0=0;\quad p_k(\zeta)=\sum_{\mu=1}^{k}\frac{\zeta^{2\mu}}{\mu},\quad k=1,2,3,\cdots.$$

We thus obtain the following integral representation for $w_k(z)$:

$$w_k(z)=-\tfrac{1}{2}z^{2-2k}\frac{1}{2\pi i}\int_\gamma dt e^t t^{3-2k}\left[\ln\left(1-\frac{z^2}{t^2}\right)+p_k\left(\frac{z}{t}\right)\right]. \quad \text{(A5)}$$

By deforming the integration path, γ, into three parts, γ_0, γ_+, and γ_-, as indicated in Fig. 4, we may express Eq. (A5) as a sum of three contributions, $w_k^{(0)}$, $w_k^{(+)}$, and $w_k^{(-)}$, corresponding to the three paths, γ_0, γ_+, and γ_-, respectively; i.e., we put

$$w_k=w_k^{(0)}+w_k^{(+)}+w_k^{(-)}.$$

By expanding the integrand in Eq. (A5) in inverse powers of z, one finds

$$w_0^{(0)}=\tfrac{1}{2}z^2(\tfrac{3}{2}-\ln\gamma);\quad w_1^{(0)}=-\tfrac{1}{4}z^2-\ln\gamma;$$

$$w_k^{(0)}=-\left[\frac{z^2}{4k}-\frac{1}{2}\frac{1}{k-1}+z^{2-2k}\Gamma(2k-2)\right],\quad k=2,3,\cdots;$$

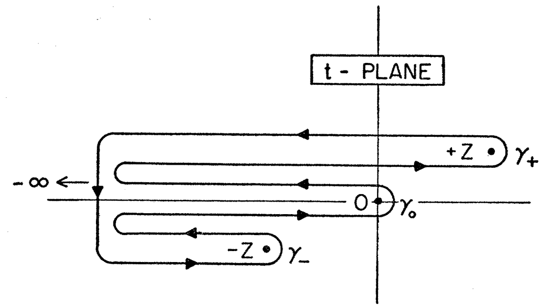

FIG. 4. Integration path γ for the integral in Eq. (A5).

and

$$w_k^{(\pm)}\approx\frac{1}{2z}\sum_{\mu=0,1,2,3,\cdots}\binom{2k-3}{\mu}\frac{\mu!}{(\mp z)^\mu},$$

$$k=0,1,2,3,4,\cdots.$$

Substituting the above expressions into Eq. (A1) and summing over k, we obtain the following semiconvergent series:

$$f^{(1)}(x;x_0)\approx\frac{2}{\sqrt{\pi}}\exp(-x^2)\left[\ln(2x_0)(2x^2-1)-\frac{1!}{(2x)^2}+\frac{3!}{(2x)^4}\mp\cdots\right]$$
$$+\frac{1}{2x\sqrt{\pi}}\left[\exp[-(x-x_0)^2]\sum_{\mu=0,1,2,\cdots}\frac{q_\mu(x_0)}{(2x)^\mu}-\exp[-(x+x_0)^2]\sum_{\mu=0,1,2,\cdots}\frac{q_\mu(x_0)}{(-2x)^\mu}\right], \quad \text{(A6)}$$

where

$$q_\mu(x_0)=(-1)^\mu\exp(x_0^2)\frac{d^\mu}{dx_0^\mu}\left(\frac{\exp(-x_0^2)}{x_0^3}\right).$$

For the case where x_0 is of the order of one, Eq. (A6) becomes for $x\gg1$

$$f^{(1)}(x;x_0)\to\frac{1}{2\sqrt{\pi}}\frac{\exp[-(x-x_0)^2]}{xx_0^3}\times\left[1+\left(x_0+\frac{3}{2x_0}\right)\frac{1}{x}+\cdots\right].$$